

Document downloaded from:

<http://hdl.handle.net/10251/40669>

This paper must be cited as:

González Martínez, A.J.; Conde, P.; Hernández Hernández, L.; Herrero Bosch, V.; Moliner Martínez, L.; Monzó Ferrer, J.M.; Orero Palomares, A.... (2013). Design of the PET–MR system for head imaging of the DREAM Project. Nuclear Instruments and Methods in Physics Research Section A: Accelerators, Spectrometers, Detectors and Associated Equipment. 702:94-97. doi:10.1016/j.nima.2012.08.028.



The final publication is available at

<http://dx.doi.org/10.1016/j.nima.2012.08.028>

Copyright Elsevier

1 **Design of the PET-MR system for head imaging of the**
2 **DREAM project**

3 A.J. González^{a,*}, P. Conde^a, L. Hernández^a, V. Herrero^a, L. Moliner^a, J.M.
4 Monzó^a, A. Orero^a, A. Peiró^a, M.J. Rodríguez-Álvarez^a, A. Ros^a, F. Sánchez^a, A.
5 Soriano^a, L.F. Vidal^a, J.M. Benlloch^a

6 ^a*Instituto de Instrumentación para Imagen Molecular (I3M). Centro Mixto UPV CSIC CIEMAT.*
7 *Camino de Vera s/n, 46022, Valencia, Spain.*

8 **Abstract**

9 In this paper we describe the overall design of a PET-MR system for head
10 imaging within the framework of the DREAM Project as well as the first detector
11 module tests. The PET system design consists of 4 rings of 16 detector modules
12 each and it is expected to be integrated in a head dedicated radio frequency coil of
13 an MR scanner.

14 The PET modules are based on monolithic LYSO crystals coupled by means of
15 optical devices to an array of 256 Silicon Photomultipliers. These types of crystals
16 allow to preserve the scintillation light distribution and, thus, to recover the exact
17 photon impact position with the proper characterization of such a distribution.
18 Every module contains 4 Application Specific Integrated Circuits (ASICs) which
19 return detailed information of several light statistical momenta. The preliminary
20 tests carried out on this design and controlled by means of ASICs have shown
21 promising results towards the suitability of hybrid PET-MR systems.

22 **Keywords:** Hybrid PET-MR, SiPM

*Instituto de Instrumentación para Imagen Molecular (I3M)
Email address: agonzalez@i3m.upv.es (A.J. González)

23 **1. Introduction**

24 It has been widely suggested the convenience of simultaneously obtain Positron
25 Emission Tomography (PET) and Magnetic Resonance (MR) images⁽¹⁾. Both sets
26 of data, if they are furthermore obtained on a dynamically mode (time dependent),
27 could provide unprecedented information on the studied disease. MR results pro-
28 vides images with higher contrast compared to the Computerized Tomography
29 (CT) and at the same time the patient avoids radiation since MR is not based on
30 x-ray sources⁽²⁾. There are many advantages of fusing PET and MR modalities,
31 but the technological challenges are still challenging. Good substitutes for the
32 conventionally used Photomultiplier Tube (PMT) technology, are the so-called
33 Silicon Photomultipliers (SiPMs)^(3,4). SiPMs are fast, have high gain, they are
34 hardly affected by magnetic fields⁽⁵⁾ and are suitable for Time of Flight (TOF)
35 measurements due to their working principle⁽⁶⁾.

36 An architectural approach to combine the PET and MR techniques within the
37 same gantry or structure, has already been suggested⁽⁷⁾. It is a very promising
38 solution since it could allow to simultaneously acquire PET and MR data. An
39 alternative approach would be the design of a PET insert, MR compatible (see
40 Fig. 1). This is specially cost effective when the MR is mainly assigned to the
41 neurology field. Note that for head explorations, the conventional whole-body
42 PET scanner is not optimized and that a dedicated one could provide higher spatial
43 resolution and sensitivity performances. A dedicated PET would also reduce the
44 scanning time of brain studies which currently last about 30 minutes.

45 This work shows the preliminary design and tests of an MR compatible PET
46 insert. This contribution is performed within the framework of the DREAM
47 Project.

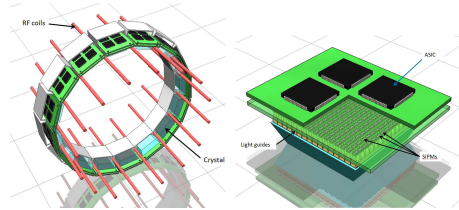


Figure 1: Drawings for the hybrid PET ring along with the brain RF coil and, the detail of one single detector module.

48 2. Material and methods

49 The PET system consists of 4 rings of 16 detector modules each and it is
 50 integrated in the head dedicated radio frequency (RF) coil of an MR system. The
 51 detector modules are designed to fit in the gaps between two wires of the RF
 52 coil (bird cage shape). In Fig. 1 a sketch of the configuration for one detector
 53 ring and one module is given. The blue blocks represent the crystals and, the
 54 black squares on top of green layers are the data control chips and their allocation
 55 boards, respectively. The RF coils can also be distinguished as red bars.

56 Based on tabulated data for human head dimensions obtained from *PeopleSize*
 57 *1999*, it was found the convenience for a transaxial field of view (FOV) of the
 58 designed system to be of at least about 206 mm in diameter. From the PET module
 59 dimensions we plan to use, and the number of allowed coincidence detector pairs,
 60 we found that 16 modules could allow one to obtain images of about 240 mm FOV
 61 size without losing significant sensitivity due to the existing gaps in between
 62 neighboring modules. In order to be able to visualize the entire brain including
 63 the hippocampus region, 4 detector rings have been suggested, covering nearing
 64 200 mm axial FOV.

65 Each detector module has been designed with the aim to be controlled by

66 means of a reduced number of Application Specific Integrated Circuits (ASICs).
67 In particular, every detector contains 4 ASICs. The main components of the de-
68 tector block are a continuous scintillator crystal, an array of solid state Silicon
69 Photomultipliers (SiPM) detectors, and the ASICs.

70 The PET modules allocate a single continuous LYSO (Cerium doped lutetium
71 based scintillation) crystal block with an entrance surface of $40 \times 40 \text{ mm}^2$ and
72 an exit face of $50 \times 50 \text{ mm}^2$, coupled to an array of 256 SiPMs of $1 \times 1 \text{ mm}^2$ area
73 each, through a matrix of light guides⁽⁸⁾. Several configurations for crystal surface
74 treatment have been studied aiming at preserving the original scintillation light
75 distribution. The most suitable solution is to black paint all crystal faces but the
76 exit one in contact with the photosensor block, in order to absorb the undesired
77 reflected light⁽⁹⁾. The thickness of the crystal is still under study in order to keep
78 a small edge effect, characteristic of continuous crystals without great penalty on
79 PET sensitivity^(10,11). A previous work⁽⁸⁾ showed that this border effect can be
80 diminished by using optical devices capable to reduce the acceptance angle (AA)
81 of the scintillation light into the photosensor.

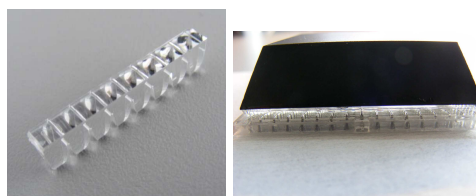


Figure 2: Photographs of the light guide array and its coupling with the scintillation crystal.

82 Different types of SiPM devices have been evaluated. In order to facilitate
83 their assembly, surface mounted device (SMD) packaging is preferable among
84 others along with a relative small active area in order to reduce the dark counts

85 (DC) contribution which squarely increases with the detection surface. Note that
86 instead of recording all SiPMs output signals (256), we will read them out with
87 ASICs in order to obtain a few parameters containing the information of the light
88 distribution, the so-called momenta. Thus, it is required to reduce the DC to avoid
89 errors in the characterization of the light distribution that could cause a loss of
90 precision in the determination of the photon impact position. Other effects like
91 temperature, SiPM breakdown voltage or its photon detection efficiency also play
92 an important role when characterizing a system that is composed of SiPMs^(12,13).
93 However, our set-up is not susceptible yet to accurately study these contributions
94 and, therefore, they are not further commented in this work.

95 Following the idea of reducing the AA at the time to focus the scintillation
96 light into the small area of the SiPM, some optical coupling devices, here called
97 light guides, were studied. The optical design of these guides has been optimized
98 using the ZEMAX simulation program that is based on light propagation within
99 the crystal and guides. An optimal configuration using parabolic surfaces was
100 found to represent a balance between light detection efficiency and cros-talk be-
101 tween channels. The system works under the total internal reflection principle.
102 Although metallic coatings such as Gold and Silver, were tested, they translated
103 into transmission losses. These guides make it possible to reduce the AA to about
104 16° , compared to 55° characteristic when the scintillation crystal is coupled to a
105 Position Sensitive Photomultiplier (PSPMT) through optical grease ($n_{LYSO}=1.82$,
106 $n_{PSPMT, borosilicate}=1.49$, $n_{grease} \approx 1.56$).

107 The selected optical configuration has already been implemented by develop-
108 ing a special cast for an array of 8 light guides using polymethyl methacrylate
109 (PMMA) as material. Figure 2 shows a real photograph of this array on the left

110 hand side. We decided to manufacture it with this configuration (1×8) to avoid
111 stratification problems due to cooling of the PMMA when injecting it into a mold.
112 A final matrix of 256 light guides was built by gluing 32 of those arrays. During
113 the simulation stage it was observed the convenience to avoid the adhesion of any
114 material in optical contact with the light guide walls in order to minimize light
115 transmission losses. The picture on Fig. 2 (right) shows the scintillation crystal
116 coupled to the array of 256 light guides.

117 *2.1. Module Readout*

118 The SiPM matrix is readout through 4 identical ASIC chips called AMIC⁽¹⁴⁾,
119 (see sketch in Fig. 1). Each AMIC reads 64 SiPM inputs and outputs up to 8
120 signals each. The AMIC chip is fully scalable: 4 AMICS are coupled together
121 to read 256 SiPMs in parallel but work as a single unit with only up to 8 output
122 signals. Each AMIC first makes up to 8 copies of the input signal from each SiPM,
123 which are then multiplied by a different constant depending on the copy and SiPM
124 position. Finally, all the input signals multiplied by the corresponding constants
125 are added, therefore forming up to 8 linear combinations of the 256 input signals.

126 Selecting the set of constants properly it allows for example the construction of
127 the different momenta of the light distribution in Cartesian coordinates, although
128 other bases of functions may be used. In such a way, the AMIC mainly serves
129 as a data reduction device that compresses the information from 256 input chan-
130 nels into up to 8 parameters describing the light distribution. Note that higher
131 orders than the second moment are hardly to be analogically implemented⁽¹⁵⁾ and,
132 therefore, the proposed approach could provide very valuable results.

133 **3. Results**

134 Some measurements were performed in order to test the feasibility of using
 135 the ASIC to read out the array of SiPMs. Here, only 64 SiPMs were used and,
 136 thus, only one ASIC was required to return the light distribution information. For
 137 these first tests, the SiPM array without the coupling light guides was mounted.
 138 The scintillator crystal had dimensions of $50 \times 50 \text{ mm}^2$ and $40 \times 40 \text{ mm}^2$ for the
 139 entrance and exit faces, respectively. The crystal thickness was 10 mm and all
 140 faces black painted but the one in contact with the SiPM array which was polished.
 141 The system was programmed to deliver the zero momentum (Energy) and, $\langle x \rangle$
 142 and $\langle y \rangle$ impact positions. All SiPMs were powered at -71.1 V, which was the
 143 lowest manufacture suggested voltage among the 64 detectors. The system was
 144 run at ambient temperature.

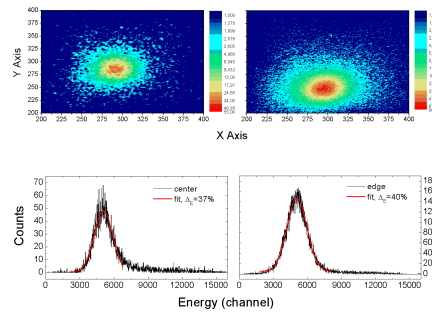


Figure 3: Top, contour plots for the acquisition of a point-like source located at the detector center and border. Bottom, energy spectra of the two acquisitions.

145 A ^{22}Na point-like source with about $1 \mu\text{Ci}$ of activity and $1 \times 1 \text{ mm}^2$ size was
 146 used in these tests. It was moved across the crystal to validate the X and Y impact
 147 photon coordinates. The source was collimated through a Tungsten pinhole of 1
 148 mm in diameter and 30 mm thickness placed just on the incoming detector surface.

149 Figure 3 depicts the acquisition of the source located at the detector center and also
150 close to the photosensor array border.

151 Since the light guides were not used, the photosensor area only covered about
152 4.9% of the total exit scintillator surface. Therefore, the determined energy reso-
153 lution was as poor as about 37% and 40% for the center and edge regions of the
154 detector block, as it can be estimated in Fig. 3 (bottom).

155 **4. Conclusions**

156 We have developed a detector module for PET-MR systems specially dedi-
157 cated to brain imaging. The module is based on a continuous scintillating crystal
158 coupled through light guides to 256 SiPMs which are read by data reduction ASIC
159 chips. The use of the light guides, due to the AA reduction, would help to increase
160 the crystal thickness without significantly worsening the image compression due
161 to border effects and, therefore, increasing the sensitivity of the PET system.

162 Preliminary results without the light guides showed the possibility of merging
163 SiPMs with ASIC devices to return valuable coincidence gamma ray (511 keV)
164 images. These results show that, even without the proper light collection, the use
165 of an ASIC allows to compute the impact coordinates. Undergoing tests have
166 delivered a depth of interaction of 3 mm resolution enabling to distinguish among
167 several virtual crystal layers and, thus, allowing to partially correct for the parallax
168 error.

169 **Acknowledgement**

170 This work was supported by the Centre for Industrial Technological Devel-
171 opment co-funded by FEDER through the Technology Fund (DREAM Project,

172 IDI-20110718), the Spanish Plan Nacional de Investigación Científica, Desarrollo
173 e Innovación Tecnológica (I+D+I) under Grant No. FIS2010-21216-CO2-01 and
174 the Valencian Local Government under Grant PROMETEO 2008/114.

175 **References**

- 176 [1] D. W. Townsend, Physical principles and technology of clinical PET imag-
177 ing, *Ann. Acad. Med. Singapore* 33 (2004) 133–145.
- 178 [2] M.S. Judenhofer *et al.*, Simultaneous PET-MRI: a new approach for func-
179 tional and morphological imaging, *Nature Medicine* 14 (2008) 459–465.
- 180 [3] S. Moehrs, A.D. Guerra, D.J. Herbert and M.A. Mandelkern, A detector head
181 design for small-animal PET with silicon photomultipliers (SiPM), *Phys.*
182 *Med. Biol.* 51 (2006) 1113–1127.
- 183 [4] D.R. Schaart, H.T. van Dam, S. Seifert, R. Vinke, P. Dendoeven, H. Löhner
184 and F.J. Beekman, A novel, SiPM-array-based, monolithic scintillator detec-
185 tor for PET , *Phys. Med. Biol.* 54 (2009) 3501–3512.
- 186 [5] S. España, L.M. Fraile, J.L. Herraiz, J.M. Udías, M. Desco and J.J. Va-
187 quero, Performance evaluation of SiPM photodetectors for PET imaging in
188 the presence of magnetic fields, *Nucl. Instrum. Meth. A* 613 (2010) 308–316.
- 189 [6] C.L. Kim, G. Wang and S. Dolinsky, Multi-Pixel Photon Counters for TOF
190 PET Detector and Its Challenges, *IEEE Trans. Nucl. Sci.* 56 (2009) 2580–
191 2585.
- 192 [7] A. Drzezga, M. Souvatzoglou, M. Eiber, A.J. Beer, S Fürst, A. Martinez-
193 Möller, S.G. Nekolla, S. Ziegler, C. Ganter, E.J. Rummeny and M.

- 194 Schwaiger, First Clinical Experience with Integrated Whole-Body PET/MR:
195 Comparison to PET/CT in Patients with Oncologic Diagnoses, *J. Nucl. Med.*
196 53 (2012) 845–855.
- 197 [8] A.J. González Martínez, A. Peiró Cloquell, F. Sánchez Martínez, L.F. Vi-
198 dal San Sebastian and J.M. Benlloch Baviera, Innovative PET detector con-
199 cept based on SiPMs and continuous crystals, *Nucl. Instrum. Meth. A*,
200 DOI:10.1016/j.nima.2011.11.029.
- 201 [9] C.W. Lerche, A. Ros, V. Herrero, R. Esteve, J.M. Monz, A. Sebasti, F.
202 Snchez, A. Munar and J.M. Benlloch, Dependency of Energy-, Position-
203 and Depth of Interaction Resolution on Scintillation Crystal Coating and
204 Geometry, *IEEE Trans. Nucl. Sci.* 55 (2008) 1344–1351.
- 205 [10] J.M. Benlloch, V. Carrilero, A.J. González, J. Catret, C.W. Lerche, D.
206 Abellán, F. García de Quirós, M. Martínez, J. Modia, F. Sánchez, N. Pavón,
207 A. Ros, J. Martínez and A. Sebastiá, Scanner calibration of a small animal
208 PET camera based on continuous LSO crystals and flat panel PSPMTs, *Nucl.*
209 *Instr. and Meth. A* 571 (2007) 26–29.
- 210 [11] F. Sánchez, J.M. Benlloch, B. Escat, N. Pavón, E. Porras, D. Kadi-Hanifi,
211 JA. Ruiz, F.J. Mora, A. Sebastiá, Design and test of portable mini gamma
212 camera, *Med. Phys* 31(6) (2004) 1384–1397.
- 213 [12] E. Roncali and S.R. Cherry, Application of Silicon Photomultipliers to
214 Positron Emission Tomography, *Ann. Biomed. Eng.* 39 (2011) 1358–1377.
- 215 [13] Y. Musienko, Advances in multipixel Geiger-mode avalanche photodiodes
216 (silicon photomultiplies), *Nucl. Instr. and Meth. A* 598 (2009) 213–216.

- 217 [14] V. Herrero-Bosch, C.W. Lerche, M. Spaggiari, R. Aliaga-Varea, N.
218 Ferrando-Jodar and Ricardo Colom-Palero, AMIC: An Expandable Front-
219 End for Gamma-Ray Detectors With Light Distribution Analysis Capabili-
220 ties, IEEE Trans. Nucl. Sci. 58 (2011) 1641–1646.
- 221 [15] C. Lerche, J. Benloch, F. Sánchez, N. Pavón, B. Escat, E. Gimenez, M.
222 Fernandez, I. Torres, M. Gimenez, A. Sebastiá and J. Martínez,, Depth of
223 gamma-ray interaction within continuous crystals from the width of its scin-
224 tillation light-distribution, IEEE Trans. Nucl. Sci. 52 (2005) 560–572.